无 机 化 学 学 报

2020 年　　第 36 卷　　第 2 期

目　次

论　文

CHINESE JOURNAL OF INORGANIC CHEMISTRY

Vol.36 No.2 Feb. 2020

CONTENTS

Cover

Articles

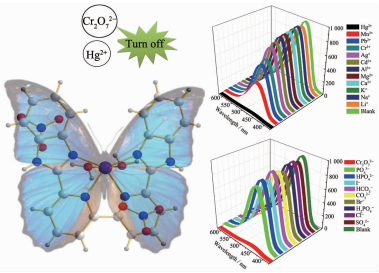

The monomeric Zn (Ⅱ) complex is butterfly-shaped and shows highly selective and sensitive detection of Hg^{2+} and $Cr_2O_7^{2-}$ in aqueous solution.

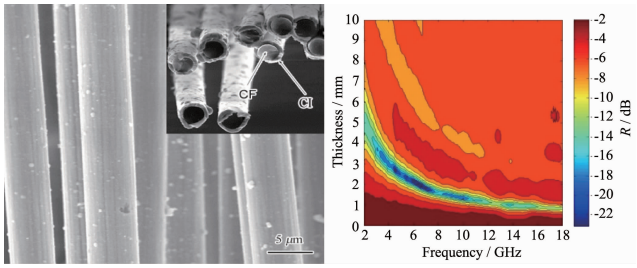

$Fe(CO)_5$ was used as precursor to construct nano-sized carbonyl iron (CI) shell on carbon fiber (CF) surface by metal organic chemical vapor deposition. The composite absorption intensity is less than −10 dB among the whole 2~18 GHz when the thickness of the coating is 0.9~3.9 mm.

Photocatalytic Degradation of Ciprofloxacin and Azo Dyes by Pt^{2+}/Pt^{0} Doped g-C_3N_4

MA Xiao-Shuai, CHEN Fan-Yun, YU Chang-Lin, YANG Kai, HUANG Wei-Ya, LI Shao-Yu

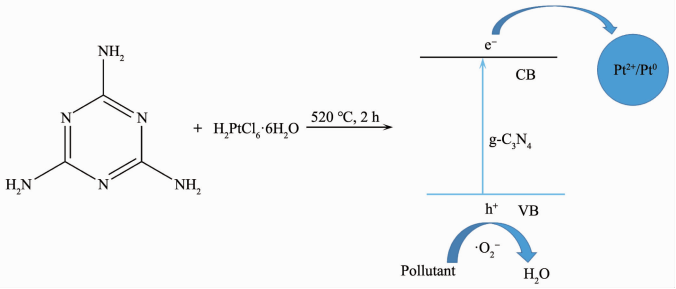

DOI:10.11862/CJIC.2020.040
Chinese J. Inorg. Chem., **2020**,**36**(2):217-225

Metal Complexes Based on 3-Nitrophthalic Acid Involving *in Situ* Decarboxylaton: Syntheses, Crystal Structures and Physical Properties

WU Guo-Zhi, WANG Peng-Fei, LI Shan-Qing, FANG Xiao-Long

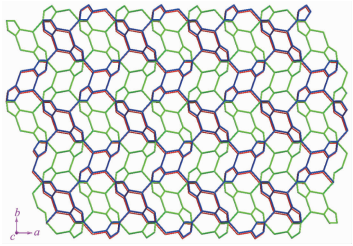

Two metal complexes, $[Zn(3\text{-}NBA)(trz)]_n$ (**1**) and $[Pb(3\text{-}NBA)(phen)_2]NO_3$ (**2**), have been constructed through hydro-thermal reaction using the 3-nitroph-thalic acid ($3\text{-}NPAH_2$) and different N-donor ligands. During the reaction, the 3-nitrobenzoic acid(3-HNBA) resulted from the *in situ* decarboxylation of the $3\text{-}NPAH_2$ ligand. In addition, the solid-state fluorescence of complexes **1**~**2** was recorded at room temperature.

DOI:10.11862/CJIC.2020.035
Chinese J. Inorg. Chem., **2020**,**36**(2):226-232

Regulation of Ligand Scale on Structure and Photocatalytic Degradation Activity of Complex: from Zero-Dimensional to One-Dimensional Cu(Ⅱ) Complexes

WANG Qi-Bao, LI Xiang, WANG Hai-Ying, LU Wen-Xin, WANG Peng

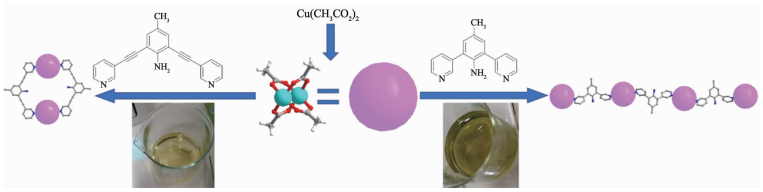

Zero-dimensional (M_2L_4 type-macrocycle) and one dimensional complexes were synthesised and showed different catalytic activity in photocatalytic degradation of methylene blue (MB). The MB was degraded faster with H_2O_2 by using macrocycle complex as catalyst than coordination polymer. This fact suggested that the properties of complexes can be affected by adjusting the size of ligands.

DOI:10.11862/CJIC.2020.043
Chinese J. Inorg. Chem., **2020**,**36**(2):233-240

Catalytic Performance of CuCo/BNNSs Nanocatalysts for Hydrolysis of Solid State Hydrogen Storage Material Ammonia Borane

ZHAI Jia-Xin, LI Guo-Hua, GAN Si-Ping, ZHANG Xue-Ming, ZHU Meng-Meng, ZHANG Xiao-Rui, HU En-Yan

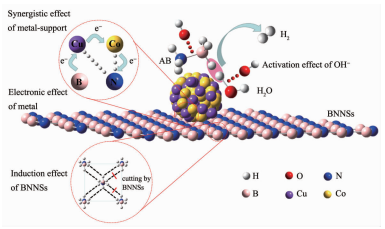

CuCo/BNNSs nanocatalyst was synthesized by co-reduction method, and the highly efficient quadruple synergistic effect between Cu, Co, BNNSs and OH^- resulted in the high catalytic activity of CuCo/BNNSs nanocatalyst towards the hydrolysis of ammonia borane.

DOI:10.11862/CJIC.2020.018
Chinese J. Inorg. Chem., **2020**,**36**(2):241-252

Preparation and Properties of Graphene-Oxide/Ag_3PO_4/Ni Composite Films with High Photocatalytic Activity under Visible Light

ZHAO Di, LIU Hong-Yan, LI Gui-Hua, LIU Yu-Yang, CUI Zi-Shuo

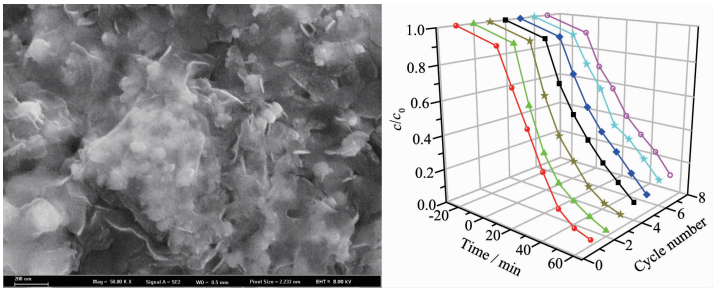

GO/Ag_3PO_4/Ni composite films prepared by electrochemical co-deposition exhibited GO-coated surface morphology outside Ag_3PO_4 nanospheres with a diameter of about 100 nm. Notably, the incorporation of GO sheets not only significantly enhanced the photocatalytic activity but also improved the structural stability of Ag_3PO_4.

DOI:10.11862/CJIC.2020.012
Chinese J. Inorg. Chem., **2020**,**36**(2):253-260

Ionothermal Synthesis of N-Deficient Graphitic Carbon Nitride with Enhanced Photocatalytic Hydrogen Evolution Activity

CUI Yan-Juan, YANG Chuan-Feng, ZHU Yu-Xin, SONG Yan-Hua, TENG Wei, TANG Sheng

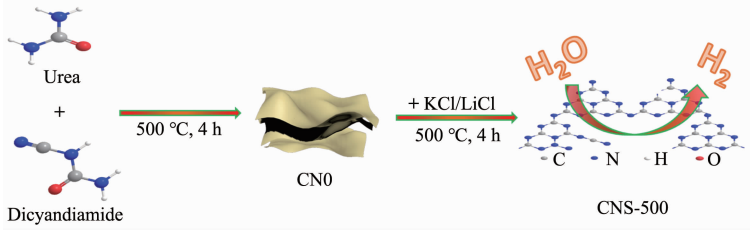

Compared to direct secondary calcination, molten salt ionothermal post-heat treatment contributed porosity, expanded light absorption and increased N-defects of g-C_3N_4, thus much enhanced photocatalytic H_2 evolution has been achieved.

DOI:10.11862/CJIC.2020.019
Chinese J. Inorg. Chem., **2020**,**36**(2):261-268

Preparation of Cathode Composites Pillar[5]quinone/CMK-3 for High-Capacity Lithium-Ion Batteries

XIONG Wen-Xu, ZHANG Xue-Qian, HUANG Wei-Wei

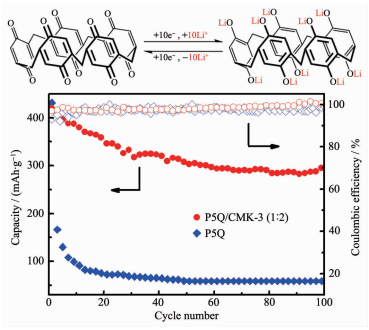

Hence, a simple ultrasonic perfusion method was used to prepare P5Q/CMK-3 nanocomposite, which reduced the contact area between P5Q and electrolyte and slowed down its dissolution. The experiment indicated the cyclic stability was great improvement of P5Q/CMK-3 nanocomposite.

DOI:10.11862/CJIC.2020.033
Chinese J. Inorg. Chem., **2020**,**36**(2):269-275

Synthesis and Luminescence Properties of Eu^{3+} doped $LaBO_3$ Phosphors

HOU Xiao-Fei, ZHAO Wan-Nan, MA Jing, SUN Ji-Qiang, LI Yan-Hong

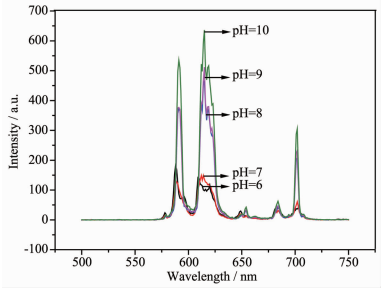

Emission intensity of the samples increased with the increase of initial solution pH value. According to the result of XRD, the three samples (pH=8, 9, 10) with orthogonal structure have higher emission intensity than that of other samples.

DOI:10.11862/CJIC.2020.016
Chinese J. Inorg. Chem., **2020**,**36**(2):276-282

Effect of Dopamine Dosages on the Microstructure and Adsorption Properties of the Fe_3O_4@PDA@PAMAM Magnetic Nano-adsorbed Materials

SUN Yi-Ming, LI Dong-Yun, SUN Yu-Kun, XU Yang, SHEN Ya-Qiang, GE Hong-Liang

DOI:10.11862/CJIC.2020.025
Chinese J. Inorg. Chem., **2020**,**36**(2):283-288

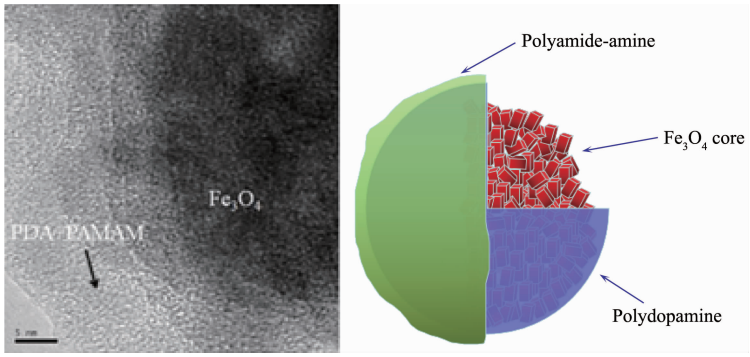

Synthesis of Small Particle Size ZSM-5 Zeolite with Kaolin by *in-Situ* Solvent Free Method

ZHANG Pei-Qing, LIU Si-Cheng, ZHENG Shu-Qin

DOI:10.11862/CJIC.2020.028
Chinese J. Inorg. Chem., **2020**,**36**(2):289-294

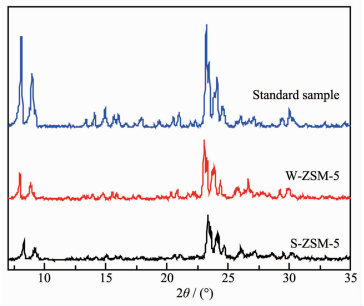

The ZSM-5 molecular sieves using natural low-cost kaolin as raw material and green synthesis without waste liquid. Not only the shortcomings of the traditional synthesis of ZSM-5 are improved, but also the synthesized samples have higher crystallinity and better performance.

Assembly of Al/Ag Nanosensor and SERS Performance for Selective Detection of Melamine with Low Concentration

CAO Lin, CHEN Qian, JIANG Fei, QIN Li-Xia, KANG Shi-Zhao, GAO Feng, LI Xiang-Qing

DOI:10.11862/CJIC.2020.050
Chinese J. Inorg. Chem., **2020**,**36**(2):295-301

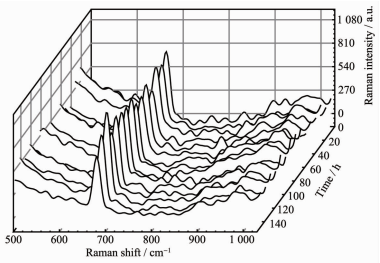

A plug-and-play Al/Ag nano surface enhanced Raman active substrate was rapidly fabricated by displacement reaction. The melamine with low concentration can be quickly and sensitively detected on the active substrate. Moreover, the substrate possesses an excellent stability and reproducibility for melamine detection.

Synthesis and Photocatalytic Activity of Monodispersed Cu_2O Micro Cubes Prepared by a Facile Methanol Thermal Reduction Method

CHEN Xiao-Ping, WEI Yuan-Song, FAN Min, SHI Jin-Ming, GUI Shuang-Lin, CHEN Bo-Hong, HUANG Shun-Nan

DOI:10.11862/CJIC.2020.027
Chinese J. Inorg. Chem., **2020**,**36**(2):302-308

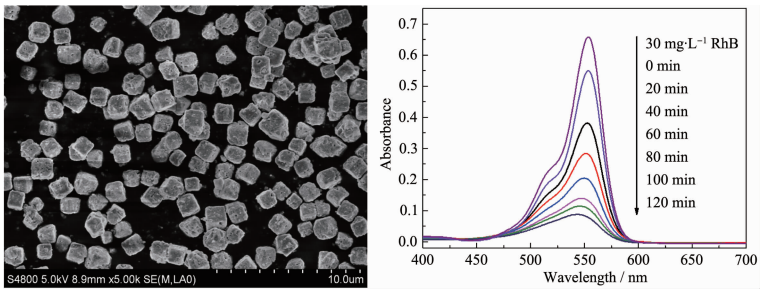

Preparation and Gas-Sensing Properties of One-Dimensional Ga_2O_3/SnO_2 Nanofibers

WU Hai-Yan, GAN Zheng-Qiang, CHU Xiang-Feng, LIANG Shi-Ming, HE Li-Fang

DOI:10.11862/CJIC.2020.021
Chinese J. Inorg. Chem., **2020**,**36**(2):309-316

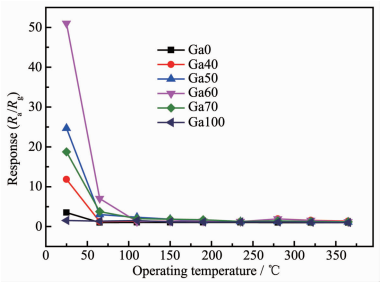

Ga_2O_3/SnO_2 nanofibers had good gas sensing selectivity and high response at room temperature (25 ℃). The response of Ga60 sensor to 1 000 μL·L^{-1} trimethylamine reached 51. The detection limit of Ga60 for trimethylamine could reach 0.8 μL·L^{-1} and the response was 1.3.

Preparation and Photocatalytic Degradation of Methylene Blue of Hierarchical Mixed-Phase Urchin-like TiO_2 Hollow Spheres

LIU Shun-Qiang, XIE Ming-Jiang, GUO Xue-Feng, JI Wei-Jie

DOI:10.11862/CJIC.2020.037
Chinese J. Inorg. Chem., **2020**,**36**(2):317-323

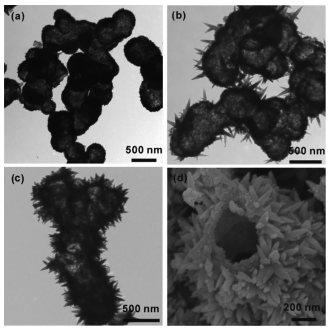

Hierarchical urchin-like TiO_2 hollow spheres comprising rutile phase of thorn and anatase phase of hollow shell was synthesized via a simple H_2O_2 assisted hydrothermal method. The density of the thorns can be effectively modified. Photocatalytic activity of the TiO_2 hollow spheres with less thorns were much better than the P25.

Electrochemiluminescence from CdS Nanocrystals@Carbon Dots Composite Film

HU Jia-Jie, ZHU Yuan, SONG Hua-Ju, WANG Ying, SHAN Yun

DOI:10.11862/CJIC.2020.034
Chinese J. Inorg. Chem., **2020**,**36**(2):324-332

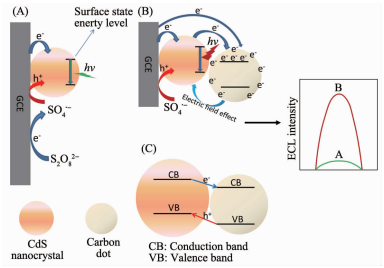

Carbon dots (CDs) can trap large numbers of electrons to generate localized electric field that facilitates formation and relaxation of excited states of neighboring CdS nanocrystals (NCs), leading to strong electrochemiluminescence from CdS NCs @CDs composite film.

Facile Solvothermal Synthesis of Porous Persimmon-like BiOBr Photocatalyst (English)

YANG Huang-Gen, CHEN Yuan, WANG Zhi-Wei, YANG Jia-Tian, ZHU Li-Gang, QIN Li-Qin, DAI Hong-Xing

DOI:10.11862/CJIC.2020.007
Chinese J. Inorg. Chem., **2020**,**36**(2):333-344

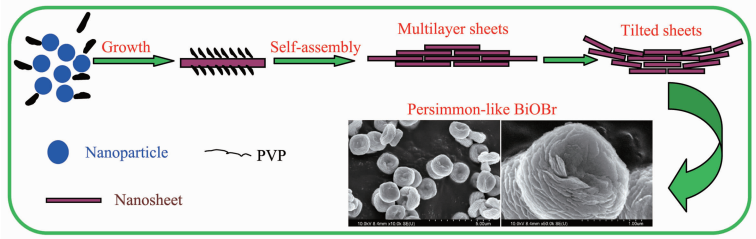

Syntheses, Crystal Structures and Magnetic Properties of Two Copper(Ⅱ) Coordination Compounds Based on 5-Bromoisophthalic Acid and 2,2′-Bipyridine (English)

LI Yu, ZOU Xun-Zhong, FENG An-Sheng, ZHAO Zhen-Yu

DOI:10.11862/CJIC.2020.002
Chinese J. Inorg. Chem., **2020**,**36**(2):345-351

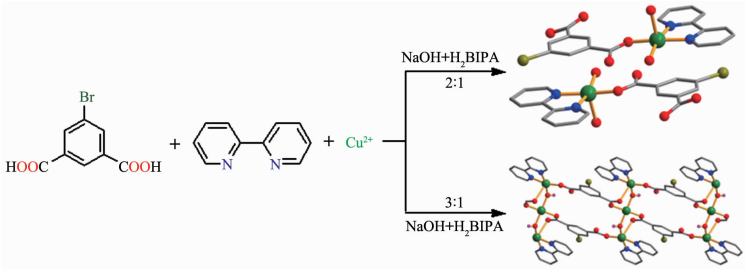

Syntheses and Spectroscopic Properties of Chiral Dinuclear Eu(Ⅲ) Complexes (English)

WANG Li-Li, YANG Qian-Ying, HAN Li-Zhi, ZHANG Xiao-Peng, CHEN Xin-Han, SHI Zai-Feng

DOI:10.11862/CJIC.2020.020
Chinese J. Inorg. Chem., **2020**,**36**(2):352-360

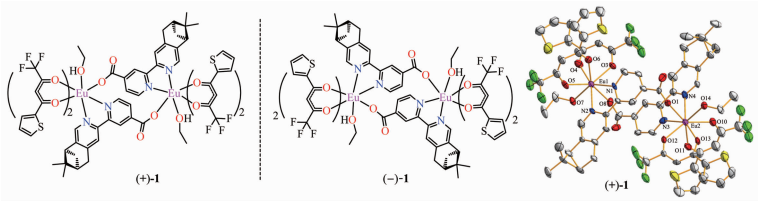

A Chiral Ag(I) Coordination Polymer Based on an α,α-*L*-Diaryl Prolinol-Pyridine Derivative: Circular Dichroism, SHG Response and Luminescent Property (English)

CHENG Lin, YANG Jing-Hua, ZHAI Qing-Chao, ZHANG Qing-Song

DOI:10.11862/CJIC.2020.013
Chinese J. Inorg. Chem., **2020**,**36**(2):361-367

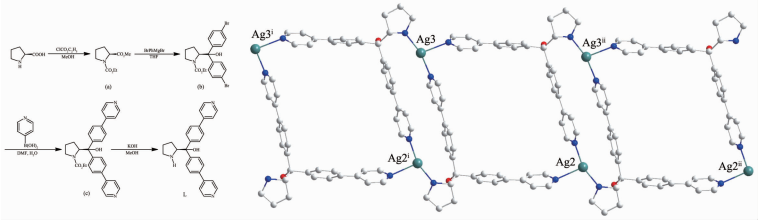

Chiral *L*-proline was used as a starting material to synthesize a pyridine-functionalized α,α-*L*-diaryl prolinol ligand, which was further applied to construct a chiral Ag(I) coordination polymer with 1D ladder-like chain structure.

Syntheses, Structures and Properties of Ni(Ⅱ)/Cd(Ⅱ)/Zn(Ⅱ) Complexes with Flexible Homophthalic Acid and Diimidazolyl-Type Ligands (Englsih)

JU Feng-Yang, LI Yun-Ping, LIU Guang-Zhen

DOI:10.11862/CJIC.2020.044
Chinese J. Inorg. Chem., **2020**,**36**(2):368-376

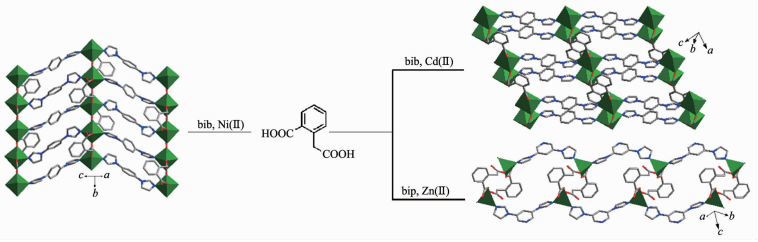

Three Ni(Ⅱ)/Cd(Ⅱ)/Zn(Ⅱ) complexes based on homophthalic acid and diimidazolyl-type ligands with structures from 1D double-stranded chain, 2D monolayer to 2D bilayer have been realized. Complex **1** exhibits typical ferromagnetic exchange coupling. And the solid state luminescences of **2** and **3** have also been given.

Syntheses, Crystal Structures, Luminescent and Magnetic Properties of 2D Manganese(Ⅱ) and Zinc(Ⅱ) Coordination Polymers Based on an Ether-Bridged Tetracarboxylic Acid (English)

LI Yu, ZHAO Zhen-Yu, ZOU Xun-Zhong, FENG An-Sheng, GU Jin-Zhong

DOI:10.11862/CJIC.2020.042
Chinese J. Inorg. Chem., **2020**,**36**(2):377-384

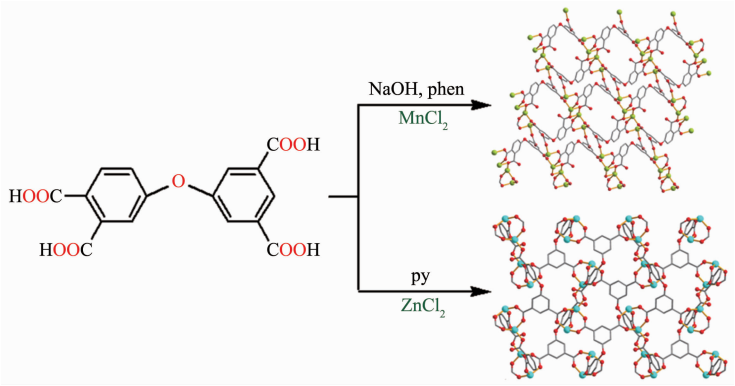

Two 2D sheet polymers, $\{[Mn_2(\mu_6\text{-L})(phen)_2]\cdot 5H_2O\}_n$ (**1**) and $\{[Zn_2(\mu_7\text{-L})(py)]\cdot H_2O\}_n$ (**2**), have been constructed, and the structures, luminescent and magnetic properties of the complexes were investigated.

Synthesis and Catalytic Performance for Oxidative Cyclization Reaction of Oil-Dispersible Core-Shell Fe_3O_4@MnO Nanocomposites (English)

YANG Qing-Xiang, LEI Li-Ling, WANG Qing-Qing, WANG Fang-Cao, WANG Cong, DONG Meng-Guo, LI Yin-Ping, CHEN Zhi-Jun

DOI:10.11862/CJIC.2020.032
Chinese J. Inorg. Chem., **2020**,**36**(2):385-391